Published in Materials Chemistry and Physics 114, issue 1, 223-227, 2009
which should be used for any reference to this work

Cherry stones as precursor of activated carbons for supercapacitors

M. Olivares-Marín[a], J.A. Fernández[b], M.J. Lázaro[c], C. Fernández-González[a], A. Macías-García[d], V. Gómez-Serrano[a], F. Stoeckli[e], T.A. Centeno[b,*]

[a] Departamento de Química Orgánica e Inorgánica, Facultad de Ciencias, Universidad de Extremadura, 06071 Badajoz, Spain
[b] Instituto Nacional del Carbón-CSIC, Apartado 73, 33080 Oviedo, Spain
[c] Instituto de Carboquímica-CSIC, Miguel Luesma Castán 4, 50018 Zaragoza, Spain
[d] Área de Ciencia de Materiales, Escuela de Ingenierías Industriales, Universidad de Extremadura, 06071 Badajoz, Spain
[e] Physics Department, University of Neuchâtel, Rue Emile Argand 11, CH-2009 Neuchâtel, Switzerland

ABSTRACT

It is shown that cherry stones-wastes can be recycled as activated carbons for electrode material in supercapacitors. KOH-activation of this precursor at 800–900 °C is an efficient process to obtain carbons with large specific surface areas (1100–1300 $m^2 g^{-1}$), average pore sizes around 0.9–1.3 nm, which makes them accessible to electrolyte ions, and conductivities between 1 and 2 $S cm^{-1}$. These features lead to capacitances at low current density as high as 230 $F g^{-1}$ in 2 M H_2SO_4 aqueous electrolyte and 120 $F g^{-1}$ in the aprotic medium 1 M $(C_2H_5)_4NBF_4$/acetonitrile. Furthermore, high performance is also achieved at high current densities, which means that this type of materials competes well with commercial carbons used at present in supercapacitors.

Keywords: Microporous materials Surfaces Adsorption Electrochemical properties

1. Introduction

The recycling of agricultural residues has received increasing attention in recent years, due to their environmental impact. A promising approach lies in the use of waste lignocellulosic materials for the production of low-cost activated carbons [1–3].

Activated carbons are porous materials obtained by treating carbonaceous solids with oxidizing gases (*e.g.* steam, air or carbon dioxide) or by carbonizing these materials following impregnation with dehydrating chemicals such as H_3PO_4, H_2SO_4, $ZnCl_2$ or KOH. Nowadays, a variety of materials with high carbon content and low quantities of inorganic compounds (coal, polymers, hard woods, coconut shell, fruit stones, *etc.*) are used as precursors [2,3].

Activated carbons consist of interconnected cavities between defective graphene layers, which result in a high degree of porosity and an extended internal surface area. It is well known that the porosity and the surface chemistry of the activated carbons depend on the raw material from which they are made and the manufacture process [2–4].

The applications of activated carbons are associated with their high porosity, being mostly used as industrial adsorbents for purification of water and of air and separation of gas mixtures. They are also used as catalytic supports and in chromatography columns [2–4].

More recently, the attention has also been focused on the development of activated carbons for specific purposes such as electrode material in electric double-layer capacitors (EDLCs) [5,6]. These devices correspond to a new type of reversible electrical energy storage systems which display high power-energy capability and long cycle life. The performance of EDLCs is based on the charging and discharging of the electrical double-layer formed by electrostatic interactions at the interface between the charged surface of an electrode and the ions of a conducting electrolyte [7].

At present, the major obstacle to the implementation of EDLC systems in a large volume market is their high cost [5,7]. The search for lower-cost carbons is a priority and lignocellulosic wastes have become interesting candidates for electrochemical applications [8–13].

In Extremadura (west-central Spain), large amounts of cherry stones are generated as waste in the industrial production of Kirsh and jam. Their removal is a major problem.

Previous studies have shown that cherry stones are an attractive source of high porosity carbons with yields similar to those reported for other fruit stones [1,14–16]. The resulting activated carbons have been used successfully for the removal of metal ions from water streams [17,18].

In order to increase the profitability of this residue, the behaviour of carbons prepared by chemical activation of cherry stones as electrodes in supercapacitors has been studied. The

---

* Corresponding author. Tel.: +34 985119090; fax: +34 985297662.
E-mail address: teresa@incar.csic.es (T.A. Centeno).

Carbon	P0.6-400	P3-400	P3-500	Z1-500	Z4-500	Z4-800	K3-500	K3-800	K3-900	K1-800
Activating agent	H_3PO_4			$ZnCl_2$			KOH			
Ratio, agent:cherry stones	0.64:1	3.44:1	3.44:1	1:1	4:1	4:1	3:1	3:1	3:1	1:1
Heat treatment temperature (°C)	400	400	500	500	500	800	500	800	900	800
Carbon yield (%)	48	47	45	39	39	38	20	12	5	15
TSA = $S_{mi} + S_e$ ($m^2\,g^{-1}$)	935	957	892	722	854	954	363	1292	1130	1273
S_{BET} ($m^2\,g^{-1}$)	946	1277	1688	567	1971	1267	279	1167	1624	1171
Conductivity ($S\,cm^{-1}$)	1.5×10^{-5}	2.1×10^{-5}	2.4×10^{-3}	1.4×10^{-6}	7.4×10^{-3}	4.5×10^{-1}	5.9×10^{-5}	1.0	2.1	1.4
Ash (% wt)	3.5	3.4	5.1	3.8	0.62	0.67	2.9	2.1	6.6	1.8

systematic use of complementary techniques for the structural, chemical and electrochemical characterization of the materials reveals the general trends in the EDLC properties of cherry stones derived-activated carbons in both aqueous (2 M H_2SO_4) and organic (1 M tetraethyl ammonium tetrafluoroborate in acetonitrile, $(C_2H_5)_4NBF_4$/AN) electrolytes. The comparison with the performance of other porous carbons, investigated by the same experimental protocols, also illustrates the potential of cherry stones derived-activated carbons as electrodes in supercapacitors.

2. Experimental

2.1. Preparation of the activated carbons

In a first step, cherry stones, as received from the "Asociación de Cooperativas del Valle del Jerte" (Cáceres, Spain), were air-dried, crushed and sieved to a particle size between 1 and 2 mm. This material was first treated with dilute H_2SO_4 solution for 24 h and subsequently washed with distilled water. This was followed by impregnation with an aqueous solution of different activating agents such as H_3PO_4, $ZnCl_2$ or KOH and heating in N_2 (100 ml min^{-1}) at a rate of 10 °C min^{-1} to temperatures between 400 and 900 °C. The soaking time at the maximum temperature was 2 h. The resulting activated carbons were washed with HCl solution and/or with distilled water until a pH of approximately 6 was obtained. The carbons were finally dried at 120 °C overnight. Details of the entire procedure are given elsewhere [14–16].

The yield of the activation process is obtained from the weights of the dry activated carbons and the H_2SO_4-washed stones.

The experimental conditions and the corresponding yields of the different activation processes are summarized in Table 1.

2.2. Analysis of the porous structure and the chemical characteristics of the carbons

The carbon porosity has been characterized by N_2 adsorption at 77 K (*Micromeritics ASAP 2010*) and by immersion calorimetry at 293 K. The theoretical background is based on Dubinin's theory for the volume filling of micropores and its extension to immersion calorimetry [4,19].

The analysis of the N_2 adsorption isotherm by Dubinin-Radushkevich equation led to the volume W_o of the micropores, their average width L_o and the surface area of their walls, S_{mi}. Moreover, the comparison of the isotherm on the given sample with the data for a non-porous reference carbon provided information on the external (non-microporous) area S_e of the carbon. The total surface area of the carbon has been estimated from TSA = $S_{mi} + S_e$.

The assessment of the micropore accessibility, on the other hand, is based on the enthalpies of immersion ($\Delta_i H$) into liquids having critical molecular sizes between 0.4 and 1.5 nm. Therefore, micropore size distributions and molecular sieve effects have been derived by using probes such as benzene (0.41 nm), cyclohexane (0.54 nm), carbon tetrachloride (0.63 nm), cyclododeca-1,5,9-triene CDDT (0.76 nm) and tri-2,4-xylylphosphate TXP (1.50 nm). These techniques have been described in detail elsewhere [19–21].

As reported elsewhere [22], the total oxygen content of the carbon surface [O] has been estimated from the enthalpy of immersion of carbon into benzene ($-\Delta_i H[C_6H_6]$) and into water ($-\Delta_i H[H_2O]$).

2.3. Electric and electrochemical measurements

The electric conductivity of the carbons was estimated from four-probe measurements in a *1260 Solartron* gain-phase analyser (frequency range 20–10^6 Hz with a voltage of 1 V). The measurements were carried out at room temperature and 741 kPa [23].

Two-electrode capacitors were assembled in Swagelok® system with pellets of comparable mass (8–10 mg) and geometric surface area of 0.5 cm^2. A glassy fibrous material played the role of separator. The electrochemical performance was studied in acidic (2 M H_2SO_4) and organic (1 M tetraethyl ammonium tetrafluoroborate in acetonitrile, $(C_2H_5)_4NBF_4$/AN)) electrolytic solutions by galvanostatic charging-discharging cycles at current densities between 1 and 100 mA cm^{-2}. Cyclic voltammetry experiments at scan rates of ranging from 1 to 50 mV s^{-1} were also performed. The cell voltage ranged from 0 to 0.8 V for aqueous medium and between 0 and 2 V for the aprotic electrolyte [20].

3. Results and discussion

3.1. Properties of the cherry stones-based activated carbons

Table 1 shows that the chemical activation of cherry stones by different agents such as H_3PO_4, $ZnCl_2$ and KOH, leads to highly porous carbons with total specific surface areas between 900 and 1300 m^2 g^{-1}. For comparison purposes, the equivalent BET-surface area is also included, although it may be misleading [20,21].

The relatively high specific surface area of cherry stones-based carbons makes them very promising for EDLCs electrodes since it allows the formation of a large double layer at electrode/electrolyte interface. However, although the surface area of the carbon electrodes is a key parameter, other factors also influence the supercapacitor performance. For example, the electric conductivity of the electrode material is of major concern, as it contributes to the reduction of the equivalent series resistance (ESR). This, in turn, increases the power capability of the supercapacitor device.

Table 1 shows that the electric conductivity of the cherry stones-based carbons is critically dependent on the carbonization temperature. The values corresponding to the materials obtained at 800–900 °C increases by at least three orders of magnitude with respect to those produced at 400–500 °C. In agreement with previous studies [6,24], heat treatment above 700 °C enhances the carbon conductivity by increasing the structural order of the pseudo-graphitic carbonaceous layers.

As expected, the cyclic voltammograms for cherry stones-based capacitors at 50 mV s^{-1} in $(C_2H_5)_4NBF_4$/acetonitrile revealed better supercapacitor performances for the high conductivity-carbons. For example, Fig. 1 shows a clear rectangular-shaped voltamogramm for the device based on carbon K3-900 with a conductivity of 2.04 S cm^{-1}. The steep current change at the switching potentials reflects quick charge propagation in the corresponding electrodes [7]. This contrasts with the high ESR and the collapsed cyclic voltammogram displayed by the item prepared with P3-500. This carbon shows only 2.4×10^{-3} S cm^{-1} of conductivity. As a consequence, the present study has been focused on cherry stones-derived carbons which combine large specific surface area and relatively high electric conductivity, such as those prepared by KOH- and $ZnCl_2$-activation at 800–900 °C.

3.2. Textural and chemical characteristics of the cherry stones-based carbons for supercapacitors

An overview of the main porous and chemical properties of the cherry stones-carbons with promising properties for supercapac-

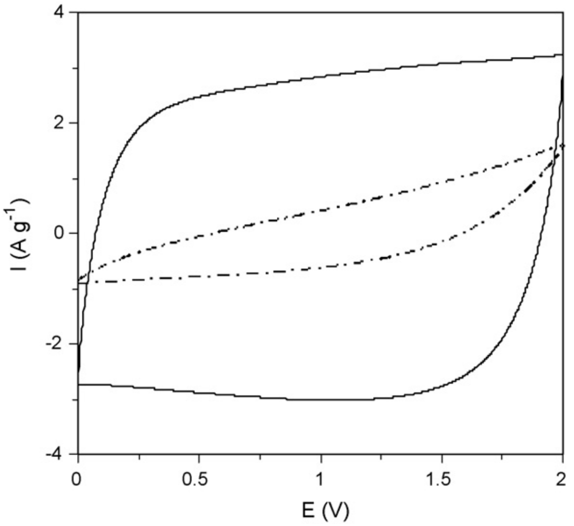

Fig. 1. Cyclic voltammograms for carbons (—) K3-900 and (- - -) P3-500 at 50 mV s^{-1} in $(C_2H_5)_4NBF_4$/acetonitrile.

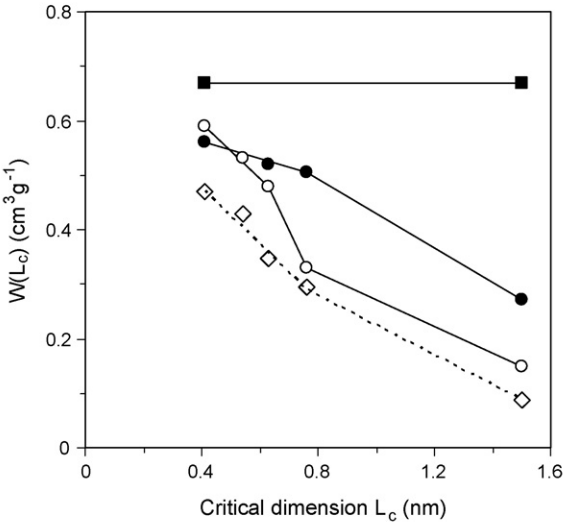

Fig. 2. Micropore volume of cherry stones-based carbons accessible to liquids with different molecular sizes: (●) K3-800; (■) K3-900; (○) K1-800; (◊) Z4-800.

itors is provided by the results of the adsorption and immersion experiments summarised in Table 2.

It appears that the porosity of the materials obtained by carbonization of a mixture of KOH and cherry stones with a ratio 3:1 at 800 and 900 °C (carbons K3-800 and K3-900) consists mainly of micropores (width <2 nm). Their surface areas are respectively 1244 m^2 g^{-1} and 1039 m^2 g^{-1}. These materials also contain a significant proportion of larger pores which lead to external (non-microporous) surfaces areas of 48 m^2 g^{-1} (K3-800) and 91 m^2 g^{-1} (K3-900).

The comparison of carbons K3-800 and K3-900 reveals a significant influence of the heat treatment temperature on the course of activation in which the micropore volume and the average micropore size are increased. Carbon K3-800 presents a micropore volume (W_o) of 0.56 cm^3 g^{-1} and an average micropore size (L_o) around 0.90 nm whereas the carbonization at 900 °C leads to a micropore volume of 0.67 cm^3 g^{-1}. In the latter case, the pore size is enlarged to 1.29 nm following the suppression of the smaller pores. The profiles of the micropore volume accessible to molecules with different critical dimensions (Fig. 2) and based on immersion calorimetry [19,21] confirm the average micropore widths, derived from the N_2 adsorption isotherm (Table 2).

On the basis of the data obtained by N_2 adsorption, it might be concluded that carbons K1-800 and K3-800 display similar porosity (Table 2) and, therefore, the influence of the KOH:carbon precursor ratio would appear to be negligible. However, immersion calorimetry with different molecular probes indicates significant differences in the micropore size distribution. In the case of carbon K1-800, the comparison of the average micropore size obtained from the adsorption isotherm (L_o = 0.96 nm) and the drop for the enthalpies of immersion into CDDT (0.76 nm) (Table 2) reflects the exclusion of these molecules from micropores compatible with their size. The presence of constrictions of approximately 0.7 nm at the entrance of the pore system reduces its accessibility and only 47% of the pores are filled by the liquid CDDT with a molecular critical dimension of 0.76 nm (Fig. 2). On the other hand, K3-800 (L_o = 0.90 nm) presents an open microporosity and 91% of the total micropore volume accomodates CDDT molecules. The different profiles in Fig. 2 clearly show that the increase in the amount of KOH increases the accessibility of the micropore system of the resulting activated carbons.

Table 2 also shows that the development of porosity by $ZnCl_2$-activation is not comparable to that achieved by using KOH. In the case of carbon Z4-800, where W_o = 0.47 cm^3 g^{-1} and L_o = 0.99 nm, the micropore surface area is 949 m^2 g^{-1} and the external surface is limited to 5 m^2 g^{-1}.

Regarding the chemical nature of carbons surface, the comparison of the enthalpies of immersion into water $\Delta_i H(H_2O)$

Table 2
Main textural and chemical characteristics of the best activated carbons derived from cherry stones.

Carbon	Z4-800	K3-800	K3-900	K1-800	SC-10	Super DLC-30
W_o (cm^3 g^{-1})	0.47	0.56	0.67	0.59	0.65	0.60
L_o (nm)	0.99	0.90	1.29	0.96	1.31	1.24
S_{mi} (m^2 g^{-1})	949	1244	1039	1224	992	968
S_e (m^2 g^{-1})	5	48	91	49	21	11
TSA = $S_{mi} + S_e$ (m^{2}g^{-1})	954	1292	1130	1273	1013	979
$-\Delta_i H[C_6H_6$, 0.41 nm] (J g^{-1})	148.0	185.5	176.1	187.0	193.9	154.7
$-\Delta_i H[C_6H_{12}$, 0.54 nm] (J g^{-1})	110.1	–	–	136.3	–	–
$-\Delta_i H[CCl_4$, 0.63 nm] (J g^{-1})	106.1	166.2	–	146.6	208.7	147.7
$-\Delta_i H$[CDDT, 0.76 nm] (J g^{-1})	77.3	142.4	–	85.6	–	–
$-\Delta_i H$[TXP, 1.50 nm] (J g^{-1})	24.0	80.4	158.5	42.8	–	–
$-\Delta_i H[H_2O]$ (J g^{-1})	42.2	62.4	70.9	62.2	45.1	37.9
$-h_i$ [H_2O] (J m^{-2})	0.044	0.048	0.063	0.049	0.044	0.039
[O] (mmol g^{-1})	1.1	2.4	3.4	2.3	0.44	0.54
[O] (μmol m^{-2} TSA)	1.2	1.9	3.0	1.8	0.43	0.55

and into benzene $\Delta_i H(C_6H_6)$ [22] suggests that the surface oxygen density for cherry stones-based materials varies between 1.2 and 3.0 μmol m^{-2}. The specific enthalpy of immersion into water, $h_i[H_2O]$ (J m^{-2}) = $\Delta_i H[H_2O]$ (J g^{-1})/TSA (m^2 g^{-1}) is around −0.04 to −0.06 J m^{-2}. (The higher values observed for K3-900 may reflect specific chemical interactions, probably due to its higher ash content.)

In summary, the physico-chemical properties of the cherry stone-derived carbons compare favourably with those observed for standard activated carbons [4,19,20,22].

3.3. Electrochemical performance of the cherry stones-based activated carbons

Fig. 3 shows general trends in the specific capacitance of activated carbons derived from different precursors and manufacture conditions [20,25–27] in both acidic (Fig. 3a) and aprotic (Fig. 3b) electrolytes. It illustrates the good correlations found between the specific capacitance at low current density (1 mA cm^{-2}) and the total surface area of cherry stones-based carbons, which corresponds to a specific surface-related capacitance [C (F g^{-1})/TSA (m^2 g^{-1})] around 0.17 F m^{-2} in H_2SO_4 electrolyte and 0.09 F m^{-2} in $(C_2H_5)_4NBF_4$/acetonitrile medium. As pointed out earlier [25–29], the higher value in the acidic electrolyte reflects extra contributions from certain functional surface complexes (containing mainly oxygen and nitrogen) in the form of quick redox reactions (pseudo-capacitance), to be added to the purely double layer capacitance associated with the surface area. In the case of the aprotic electrolyte, the contribution does practically not depend on the chemistry of the carbon surface [26,27].

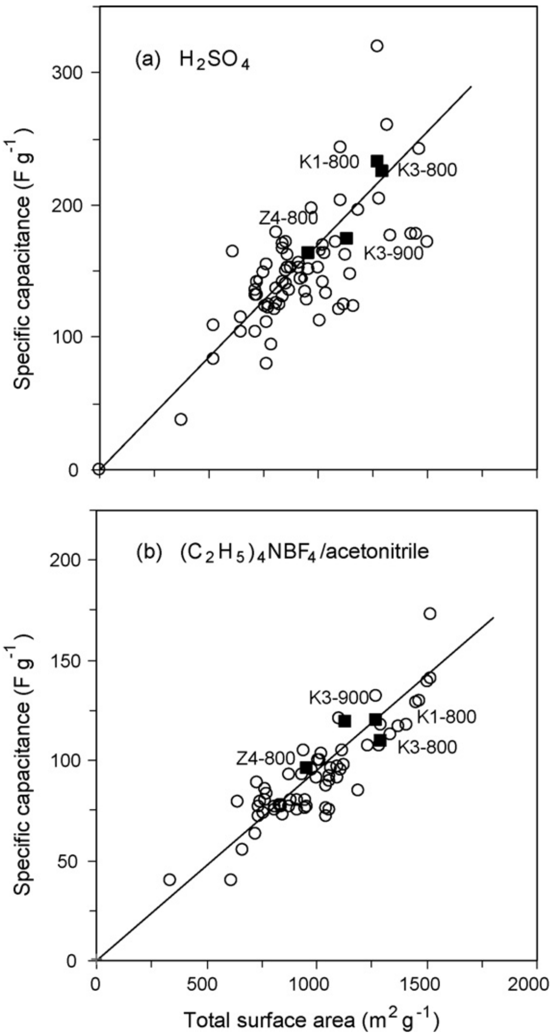

Fig. 3. Variation of the specific capacitance at 1 mA cm^{-2} in H_2SO_4 electrolyte, with the total surface area of a large variety of porous carbons in (a) 2 M H_2SO_4 and (b) 1 M $(C_2H_5)_4NBF_4$ in acetonitrile: (■) cherry stones derived-activated carbons, (○) typical activated carbons [20,25–27]. The line through the origin corresponds to a linear best fit for the cherry stones-based carbons.

Table 3
Electrochemical properties for the best activated carbons derived from cherry stones and activated carbons commercialized for supercapacitor devices.

Carbon	Specific capacitance			
	H_2SO_4		$(C_2H_5)_4NBF_4$/acetonitrile	
	F g^{-1} [a]	F cm^{-3} [b]	F g^{-1} [a]	F cm^{-3} [b]
Z4-800	163	67.4	96	39.7
K3-800	225	86.1	110	42.1
K3-900	174	64.1	119	43.8
K1-800	232	87.0	120	45.0
SC-10	165	54.2	100	32.9
Super DLC-30	156	61.5	95	37.4

[a] Referred to the carbon mass in a single electrode.
[b] Referred to the electrode volume.

For the KOH-activated cherry stones the limiting gravimetric capacitances (expressed per carbon mass of one electrode) are as high as 230 F g^{-1} in the H_2SO_4 electrolyte and 120 F g^{-1} in the $(C_2H_5)_4NBF_4$/acetonitrile medium. These values are close to the upper bounds found for standard activated carbons [25–27] (Fig. 3a and b), and surpass those achieved by lignocellulosic wastes derived-activated carbons commercialized for supercapacitor devices, such as SC-10© [Arkema-Ceca (France)] and Super DLC-30© [Norit, The Netherlands] (Table 3). Furthermore, the somewhat higher volumetric capacitance (Table 3) enhances the industrial potential of the cherry stones-based carbons for small electric power sources.

The so-called Ragone plots shown in Fig. 4 confirm the promising features of activated carbons prepared from cherry stones to be

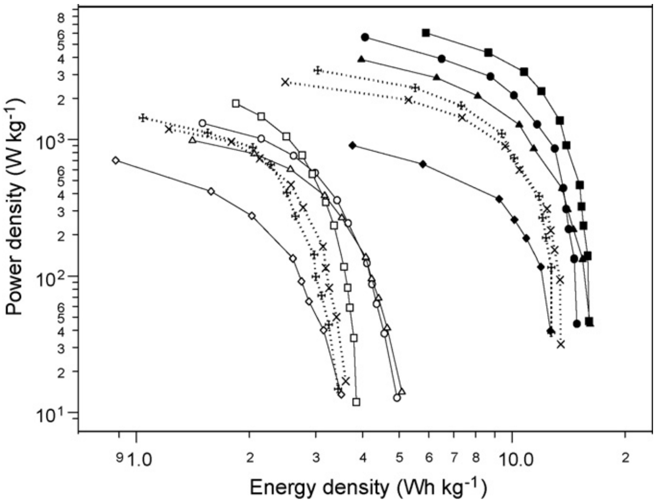

Fig. 4. Power density *vs.* Energy density for cherry stones-derived carbons: K3-800 (○, ●); K3-900 (□, ■); K1-800 (△, ▲); Z4-800 (◊, ♦). Commercial activated carbons SC-10 (X) and Super DLC-30 (+) are included for comparison. The data corresponds to unit mass of carbon in the capacitor. Open symbols for 2 M H_2SO_4 aqueous solution. Closed symbols for 1 M $(C_2H_5)_4NBF_4/CH_3CN$.

used as electrodes in both aqueous and aprotic supercapacitors. A comparative evaluation suggests that capacitors built with carbons obtained by KOH-activation at 800–900 °C are more advantageous for the release of the stored electric energy, compared with the two standards (SC-10 and Super DLC-30).

Due to its relatively high surface area, the energy stored at low discharge rate by carbon prepared with $ZnCl_2$-800 °C compares with that of the commercial carbons but, this material is not a good option for high power applications since the energy density drops with increasing power output (Fig. 4).

One observes a quite different behaviour for carbon K3-800, which provides about $4\,Wh\,kg^{-1}$ at $5500\,W\,kg^{-1}$ for $2\,V$-$(C_2H_5)_4NBF_4/CH_3CN$ devices, whereas it achieves power density around $1500\,W\,kg^{-1}$ at $1\,Wh\,kg^{-1}$ in the $0.8\,V$-H_2SO_4 system. A somewhat better performance is observed for carbon K3-900 (Fig. 4), but considerations based on production costs (higher temperature required for its production and the lower carbon yield) make it less competitive than K3-800 (Table 1).

4. Conclusions

The conversion of waste cherry stones to activated carbons for electrode material in high-performance supercapacitors offers significant potentials for reducing the cost and the environmental damage resulting from uncontrolled disposal of this residue.

KOH-activation of cherry stones at 800–900 °C appears to be an effective process to produce carbons with large specific surface area (1100–$1300\,m^2\,g^{-1}$), a porosity accessible to electrolyte ions (average micropore sizes around 0.9–1.3 nm) and high electric conductivity (1–$2\,S\,cm^{-1}$). These combined features lead to capacitances at low current density as high as $230\,F\,g^{-1}$ in the $2\,M$ H_2SO_4 aqueous electrolyte and $120\,F\,g^{-1}$ in the aprotic medium $1\,M$ $(C_2H_5)_4NBF_4$/acetonitrile. Furthermore, high performances can also achieved at high current densities. Typically, at a power density of 5500–$6000\,W\,kg^{-1}$ one obtains an energy density around 4–$6\,Wh\,kg^{-1}$ for $2\,V$-$(C_2H_5)4NBF_4/CH_3CN$ devices. For the $0.8\,V$-H_2SO_4 devices, at 1500–$2000\,W\,kg^{-1}$ the energy density is 1–$2\,Wh\,kg^{-1}$.

The comparative analysis carried out under the same experimental protocols shows that the capacitors built with carbons obtained by KOH-activation at 800–900 °C are more advantageous for the release of the stored electric energy, compared with the standards SC-10 and Super DLC-30 commercialized for supercapacitors.

Acknowledgements

Financial support from the Ministerio de Educación y Ciencia (project BQU2002-03600) of Spain is gratefully acknowledged. The authors wish to thank NORIT and ARKEMA-CECA for the gift of carbons Super DLC-30 and SC-10, respectively.

References

[1] O. Ioannidou, A. Zabaniotou, Renew. Sust. Energ. Rev. 11 (2007) 1966.
[2] H. Marsh, F. Rodriguez-Reinoso, Activated Carbon, Elsevier, Ámsterdam, 2006.
[3] F. Rodríguez-Reinoso, in: F. Schüth, K.S.W. Sing, Weitkamp (Eds.), Handbook of Porous Solids, Wiley-VCH, GmBh, Weinham, 2002, p. 1766.
[4] R.C. Bansal, J.B. Donnet, F. Stoeckli, Active Carbon, Marcel Dekker, New York, 1988.
[5] A. Burke, Electrochim. Acta 53 (2007) 1083.
[6] A.G. Pandolfo, A.F. Hollenkamp, J. Power Sources 157 (2006) 11.
[7] B.E. Conway, Electrochemical Supercapacitors, Kluwer Academic, New York, 1999.
[8] Y. Guo, J. Qi, Y. Jiang, S. Yang, Z. Wang, H. Xu, Mater. Chem. Phys. 80 (2003) 704.
[9] S. Hirahara, Y. Takeda, K. Toki, US Patent 2002/0114126 (2002).
[10] C.C. Hu, C.C. Wang, F.C. Wu, R.L. Tseng, Electrochim. Acta 52 (2007) 2498.
[11] Y.J. Kim, B.J. Lee, H. Suezaki, T. Chino, Y. Abe, T. Yanagiura, K.C. Park, M. Endo, Carbon 44 (2006) 1592.
[12] M. Okamura, M. Takeuchi, US Patent 2002/0012223 (2002).
[13] F.C. Wu, R.L. Tseng, C.C. Hu, C.C. Wang, J. Power Sources 138 (2004) 351.
[14] M. Olivares-Marín, C. Fernández-González, A. Macías-García, V. Gómez-Serrano, Appl. Surf. Sci. 252 (2006) 5980.
[15] M. Olivares-Marín, C. Fernández-González, A. Macías-García, V. Gómez-Serrano, Appl. Surf. Sci. 252 (2006) 5967.
[16] M. Olivares-Marín, C. Fernández-González, A. Macías-García, V. Gómez-Serrano, Energy Fuel 21 (2007) 2949.
[17] M. Olivares-Marín, C. Fernández-González, A. Macías-García, V. Gómez-Serrano, Adsorption, in press, doi:10.1007/s10450-008-9111-3.
[18] J. Jaramillo, V. Gómez-Serrano, P.M. Álvarez, J. Hazard. Mater 14 (2008) 601.
[19] F. Stoeckli, in: J. Patrick (Ed.), Porosity in Carbons-Characterization and Applications, Arnold, London, 1995, p. 67.
[20] T.A. Centeno, F. Stoeckli, in: V. Gupta (Ed.), Recent Advances in Supercapacitors, Transworld Research Network, Kerala, 2006, p. 57.
[21] F. Stoeckli, T.A. Centeno, Carbon 43 (2005) 1184.
[22] F. Stoeckli, A. Lavanchy, Carbon 38 (2000) 475.
[23] J. Sánchez-González, A. Macías-García, M.F. Alexandre-Franco, V. Gómez-Serrano, Carbon 43 (2005) 741.
[24] C.A. Leon, D. Leon, L.R. Radovic, in: P.A. Thrower (Ed.), Chemistry and Physics of Carbon, vol. 24, Marcel Dekker, New York, 1994, p. 213.
[25] T.A. Centeno, F. Stoeckli, Electrochim. Acta 52 (2006) 560.
[26] T.A. Centeno, M. Hahn, J.A. Fernández, R. Kötz, F. Stoeckli, Electrochem. Commun. 9 (2007) 1242.
[27] G. Lota, T.A. Centeno, E. Frackowiak, F. Stoeckli, Electrochim. Acta 53 (2008) 2210.
[28] M.J. Bleda-Martínez, J.A. Maciá-Agulló, D. Lozano-Castelló, E. Morallón, D. Cazorla-Amorós, A. Linares-Solano, Carbon 43 (2005) 2677.
[29] M.J. Bleda-Martínez, D. Lozano-Castelló, E. Morallón, D. Cazorla-Amorós, A. Linares-Solano, Carbon 44 (2006) 2642.